Inorganic chlorine variability in the Antarctic vortex and implications for ozone recovery

S.E. Strahan[1,2], A.R. Douglass[2], P.A. Newman[2], and S.D. Steenrod[1,2]

[1]Goddard Earth Sciences Technology and Research, Universities Space Research Association, Columbia, MD

[2]NASA Goddard Space Flight Center, Greenbelt, MD

Corresponding Author: Susan E. Strahan, Code 614, NASA Goddard Space Flight Center, Greenbelt, MD, 20771 (susan.e.strahan@nasa.gov)

Accepted Article

This article has been accepted for publication and undergone full peer review but has not been through the copyediting, typesetting, pagination and proofreading process which may lead to differences between this version and the Version of Record. Please cite this article as doi: 10.1002/2014JD022295

©2014 American Geophysical Union. All rights reserved.

Abstract

We infer the interannual variability of inorganic chlorine in the Antarctic lower stratospheric vortex using nine years of Aura Microwave Limb Sounder (MLS) nitrous oxide (N_2O) measurements and a previously measured compact correlation. Inorganic chlorine (Cl_y) is the sum of the destruction products of long-lived chlorine-containing source gases. Its correlation with N_2O, derived from observations in the year 2000, is scaled to the years 2004-2012 to account for subsequent N_2O growth and chlorofluorocarbon decline. The expected annual Cl_y change due to the Montreal Protocol is -20 ppt/yr, but the MLS-inferred Cl_y varies year-to-year from -200 to +150 ppt. Because of this large variability, attributing Antarctic ozone recovery to a statistically significant chlorine trend requires 10 years of chlorine decline. We examine the relationship between Equivalent Effective Stratospheric Chlorine (EESC) and ozone hole area. Temperature variations driven by dynamics are a primary contributor to area variability, but we find a clear linear relationship between EESC and area during years when Antarctic collar temperatures are 1σ or more below the mean. This relationship suggests that smaller ozone hole areas in recent cold years 2008 and 2011 are responding to decreased chlorine loading. Using ozone hole areas from 1979-2013, the projected EESC decline, and the inferred interannual Cl_y variability, we expect ozone hole areas greater than 20 million km^2 will occur during very cold years until 2040. After that time, all ozone hole areas are likely to be below that size due to reduced EESC levels.

Key points (80 characters max):

Antarctic inorganic chlorine (Cl_y) variability is inferred from N_2O, 2004-2012

Interannual Cl_y variability can be ±10 times greater than its expected decline

The Antarctic ozone hole will still be large during very cold years until 2040

Accepted Article

©2014 American Geophysical Union. All rights reserved.

1. Introduction

The Antarctic ozone hole, first reported by Farman et al. [1985], has been an annual feature of the stratosphere for more than 30 years. Its area depends primarily on inorganic chlorine (Cl_y) and temperature in the polar vortex [Newman et al., 2004]. From 1980 to 1992, the lower stratospheric Cl_y abundance nearly doubled and the ozone hole area, as measured by the area with column O_3 less than 220 Dobson Units (DU), grew from less than 2 to greater than 20 million km^2 (M km^2). During the 1990s, Cl_y growth slowed and then ceased due to the effects of the Montreal Protocol and its amendments and adjustments that regulated production of ozone-depleting substances (ODSs), the sources of most stratospheric Cl_y. The decline of Cl_y since the early 2000s has been confirmed by column measurements of $ClONO_2$ and HCl, the primary components of lower stratospheric Cl_y, and by satellite observations of HCl in the upper stratosphere, where it represents ~100% of Cl_y [Rinsland et al., 2003; Froidevaux et al., 2006]. The ozone hole area also ceased its rapid growth by the mid-1990s and since then its annual size variations have been dominated by dynamically driven temperature variations near the vortex edge or 'collar' region, 60-75°S. Lower temperatures there lead to increased surface area on sulfate aerosol and polar stratospheric cloud particles, increasing heterogeneous phase conversion of chlorine reservoir species into reactive chlorine species, i.e., ClO_x. This chlorine activation increases ozone loss and the area of the ozone hole [Kawa et al., 1997; Newman et al., 2004, 2006].

Numerous methods have been used to diagnose the severity of the Antarctic ozone hole, including the spring minimum column O_3, the time-averaged area with column O_3 less than 220 DU [Uchino et al., 1999; Newman et al., 2004], the October mean column O_3 from 63°-90°S [WMO, 2003], and the ozone mass deficit [Uchino et al., 1999; Bodeker et al., 2005; Huck et al., 2007]. The 220 DU choice represents a value lower than most ground-based observations prior to the first appearance of the ozone hole. It typically occurs within a sharp

©2014 American Geophysical Union. All rights reserved.

Accepted Article

column gradient region, making the area fairly insensitive to this choice or instrument calibration. The ozone mass deficit or deficiency (OMD) calculates an ozone mass loss relative to a column O_3 from a pre-ozone hole period, e.g., before 1976 [Uchino et al., 1999], but can also be calculated with respect to 220 DU [Bodeker et al., 2005]. Because it counts all molecules of O_3 lost within a given spatial and temporal range, the OMD may be a more sensitive diagnostic of ozone loss than the <220 DU area definition. Bodeker et al. [2005] found that OMDs increased significantly in the 1990s while Newman et al. [2004] reported that the area with less than 220 DU O_3 levelled off by the early 1990s.

Whether defined by the area with column O_3 less than 220 DU or by OMD, the Antarctic ozone hole first appeared around 1980. It is expected to disappear this century as ODSs decline. Projections from chemistry climate models (CCMs) for the return to 1980 October Antarctic column O_3 span a 40-year range that begins in the next decade [Strahan et al., 2011]. However, the CCMs' return to their simulated 1980 ozone levels is not synonymous with the disappearance of the ozone hole; the majority of CCMs continue to produce hole areas of 5-10 M km^2 until 2080 [SPARC, 2010]. Newman et al. [2006] used a parametric fit of ozone hole areas to Cl_y and Br_y abundance and temperature to project how the area will decline as halogen loading decreases. An updated version of this parametric projection predicts that a decrease in area due to declining halogens, distinguishable from the effects of temperature variability, will occur between 2015 and 2033 [Kramarova et al., 2014], with full recovery (i.e., zero area) occurring 40-50 years later.

The recovery of Antarctic ozone is slow because the lifetimes of the major ODSs CFC-11 ($CFCl_3$) and CFC-12 (CF_2Cl_2) are long, 52 and 102 yrs respectively [SPARC, 2013], resulting in a Cl_y decline rate of less than 1%/yr. Because ozone depletion depends on abundances of both inorganic chlorine and bromine, the concept of Equivalent Effective Stratospheric Chlorine (EESC) was developed to quantify their combined destructive

©2014 American Geophysical Union. All rights reserved.

Accepted Article

potential [Daniel et al., 1995; WMO, 2003]. Newman et al. [2007a] use a formulation for EESC that takes into account the altitude-dependent release of Cl and Br from organic halocarbons during stratospheric transport (i.e., fractional release) to project the decline of EESC and Cl_y in the 21st century. They estimate that EESC has declined nearly 200 ppt between 2004 and 2013 (~0.8%/yr) in the lower stratosphere Antarctic vortex for potential temperatures between ~400-500 K where mean age is ~4.5-5.8 yrs. While a global decline in HCl of 0.8 %/year has been detected above the stratopause [Froidevaux et al., 2006] and in HCl and $ClONO_2$ columns [Rinsland et al., 2003], there are no vertically resolved lower stratospheric measurements of all the Cl_y components (i.e., HCl, $ClONO_2$, Cl_2O_2, ClO, etc.) inside the Antarctic spring vortex that quantify the decline at the levels where most ozone depletion occurs.

Many of the Cl-containing species produced from photolysis of chlorofluorocarbons (CFCs) have short photochemical lifetimes but their sum, Cl_y, is conserved and can be treated as a long-lived trace gas. Stratospheric transport and its variability play a key role in determining Cl_y distributions [Waugh et al., 2007]. Nitrous oxide (N_2O) is a long-lived trace gas emitted at the surface with a lifetime of more than one year outside the tropics at altitudes below 30 hPa. Kawa et al. [1992] used the compact correlation they found between N_2O and the long-lived CFCs measured during two aircraft campaigns to estimate Cl_y mixing ratios in the Arctic and Antarctic lower stratosphere. Plumb and Ko [1992] explained that the observed compact correlations were expected, including the one derived between N_2O and Cl_y, because the timescale for isentropic transport is shorter than the species' local photochemical lifetimes. Plumb [2007] expanded the theoretical understanding of tracer correlations, showing why distinct correlation curves occur in tropical, middle, and polar latitudes. Other aircraft studies continued the use of the compact correlation between N_2O and CFCs to calculate inorganic chlorine [Woodbridge et al., 1995; Schauffler et al., 2003]. The Schauffler

©2014 American Geophysical Union. All rights reserved.

Accepted Article

study used aircraft data from a comprehensive set of organic chlorine measurements and N_2O to calculate Cl_y as a function of N_2O over the range of 50-315 ppb.

In this study, we infer inorganic chlorine variability inside the Antarctic lower stratospheric vortex for 2004-2012 using N_2O observations from the Microwave Limb Sounder (MLS) and the compact relationship between N_2O and Cl_y derived from observations by Schauffler et al. [2003]. The observations and a supporting chemistry transport model simulation are introduced in Section 2. In Section 3 we present MLS N_2O observations inside the Antarctic vortex and show the methodology used for scaling the Schauffler et al. [2003] relationship to the Aura observation period. Our results provide an observationally-derived assessment of vortex-averaged Cl_y variability at levels where Antarctic ozone depletion occurs. In Section 4 we examine the relationship between EESC and ozone hole area, a metric of the severity of ozone depletion [WMO, 2003]. In Section 5, we use a metric for Antarctic collar temperatures to identify the relationship between EESC and ozone hole area during very cold years. Using this relationship, the projected decline in EESC in the coming decades, and the observed interannual variability of Cl_y, we estimate when the ozone hole will be consistently smaller than 20 M km^2.

2. Observations and the GMI Simulation

Aura MLS version 3.3 Level 2 measurements of N_2O and temperature in the lower stratosphere (46.4, 68.1 and 100 hPa) are used in this analysis. The accuracy of v3.3 N_2O is unchanged from version 2.2 [Livesey et al., 2011; Lambert et al., 2007] and its vertical resolution is ~4 km. The estimated 2σ accuracy of N_2O data is 13% for 46 and 68 hPa retrievals and 25% for the 100 hPa data; correlative data from the SCISAT-1 Atmospheric Chemistry Experiment (ACE) instrument [Strong et al., 2008] agree with MLS values within ±5% at these pressure levels. The primary band for MLS N_2O retrievals failed on June 6, 2013, and subsequent profiles retrieved using a different band are noisier and high biased at

©2014 American Geophysical Union. All rights reserved.

Accepted Article

100 hPa compared to measurements using the primary band [A. Lambert, pers. comm.]. For this analysis we limit observations to 2004-2012, before band failure.

We use Antarctic ozone hole area data from 1979-2013 to investigate their relationship to EESC abundance. The area data were obtained from the NASA Ozone Watch website (http://ozonewatch.gsfc.nasa.gov/meteorology/annual_data.html). Ozone hole areas are calculated as the area inside the 220 DU contour of satellite-measured total column O_3 [Newman et al., 2004].

To demonstrate the global nature of the compact correlation between N_2O and Cl_y we use the Global Modeling Initiative (GMI) chemistry and transport model (CTM) integrated with 1^ox1.25^o horizontal resolution meteorological fields from the Modern Era Reanalysis for Research and Applications (MERRA) [Rienecker et al., 2011; Strahan et al., 2013]. The GMI CTM has been integrated from 1990-2013 with realistically changing source gas boundary conditions for N_2O and the CFCs. Strahan et al. [2013] evaluated GMI-MERRA transport in the Arctic lower stratosphere and showed excellent agreement between simulated and observed N_2O distributions. They demonstrated that important high latitude stratospheric transport processes - polar descent and isolation – were well-represented in this simulation.

3. N_2O and Inferred Inorganic Chlorine in the Antarctic Vortex

3.1 Lower Stratospheric N_2O in the Late September Vortex

MLS N_2O measurements inside the Antarctic vortex during spring show large year-to-year variability. Figure 1 shows the full range of the variability on the 450 K isentropic surface (~50-70 hPa). The lowest N_2O values were observed in 2005, when large areas inside the vortex had less than 90 ppb (Fig. 1a), and the highest values were observed in 2011, when few mixing ratios were less than 110 ppb (Fig. 1b). The vortex edge, shown in white, was

©2014 American Geophysical Union. All rights reserved.

Accepted Article

determined using MERRA potential vorticity (PV) and the location of the steepest PV gradients on an isentropic surface [Nash et al., 1996]. Figure 1c shows the frequency distributions of N_2O mixing ratios inside the vortex at 450 K for the period 21-30 September for each year of observations. The vortex is intact and well-defined on these dates in all years shown. Three of the years (2005, 2007, and 2009) have similar, low N_2O distributions with maxima near 95 ppb. One year, 2011, has a singularly high distribution with a broad peak centered near 130 ppb, and the remaining five years are similar to each other and have maxima near 110 ppb. Typical year-to-year variations are about 20 ppb. The approximately biennial variations suggest that the Quasi-Biennial Oscillation (QBO) influences vortex composition. Hofmann et al. [1997] speculated that the quasi-biennial variations in ozone loss rates they calculated from ozone sonde data might be driven by QBO variations in the transport of halogens to the Antarctic. Transport variations that affect halogens would similarly affect other long-lived species such as N_2O.

Figure 2 shows the year-to-year variations in vortex mean N_2O on the 450 K surface, calculated from the mean values of each MLS N_2O distribution in Fig. 1c. The dashed line in Figure 2 shows the time series of vortex mean N_2O variability simulated by the GMI CTM. The simulated year-to-year variability agrees closely with the observations and has a correlation of 0.95 with the observed time series. Lower stratospheric N_2O is controlled by transport and the GMI simulation integrated with the MERRA reanalysis credibly represents the interannual variations of transport by the Brewer-Dobson circulation during the Aura period.

3.2 The Compact Correlation Between N_2O and Cly, 2000-2012

Nitrous oxide and CFCs are emitted at the surface. They enter the stratosphere in the tropics and are slowly transported upward by the Brewer-Dobson circulation. In the middle and upper stratosphere, N_2O is destroyed primarily by photolysis but also by reaction with $O(^1D)$,

©2014 American Geophysical Union. All rights reserved.

Accepted Article

which leads to production of odd nitrogen (NO_y).CFCs are destroyed by photolysis, producing Cl_y [Hall et al., 1999]. Below 30 hPa the local photochemical lifetimes of N_2O and the CFCs in the extratropics are long (~years) while the timescale for isentropic mixing is much shorter (~months). This produces a compact tracer-tracer relationship between N_2O and long-lived CFCs, and additionally, between N_2O and Cl_y, the product of CFC destruction. The subtropical and polar mixing barriers result in distinct tracer-tracer curves for the tropics, middle, and high latitudes [Plumb, 2007].

Using comprehensive measurements of organic halocarbons and N_2O in the 50-315 ppb range inside and outside the Arctic vortex, Woodbridge et al. [1995] and Schauffler et al. [2003] each found a single, compact relationship between N_2O and Cl_y, not separate curves for mid and polar latitudes as described by Plumb [2007]. This can be understood by considering the range of N_2O values found in the mid and high latitude lower stratosphere. The winter N_2O climatology derived from a decade of lower stratospheric aircraft observations in the Arctic and Antarctic [Strahan et al., 1999] shows that between 400-500 K (~100-40 hPa), N_2O values below 180 ppb are only found inside the vortex. The compact correlations found by Schauffler and Woodbridge can be thought of as two correlation curves, for midlatitude and vortex air, that meet near 180 ppb N_2O. The transition between the mid and high latitude correlations is suggested by Figure 5 of Woodbridge et al. [1995], which shows increased compactness of the N_2O and organic halocarbons (CCl_y) relationship where $N_2O < 180$ ppb; Figure 7 of Schauffler et al. [2003] shows a transition between two different slopes in the N_2O/Cl_y curve that occurs between 170-190 ppb N_2O.

The compact correlation between N_2O and Cl_y can be used to infer Cly variability inside the Antarctic vortex from MLS N_2O observations. Because the relationship determined in Schauffler et al. [2003] used lower stratospheric measurements in the Arctic, we first show that the compact correlation is also valid in the Antarctic. This is accomplished using a GMI

©2014 American Geophysical Union. All rights reserved.

Accepted Article

CTM simulation. In addition, because N_2O has increased and CFCs have declined since 2000, the correlation must be scaled for the period of the MLS measurements, 2004-2012.

We compare the Schauffler relationship with N_2O and Cl_y from the GMI simulation in the year 2000 to show that the same correlation curve is found in both hemispheres. The top panels of Figure 3 show the GMI N_2O/Cl_y correlations between 400-500 K in southern and northern latitudes poleward of 50^o (black) and compare them to the relationship determined from lower stratospheric observations 52-88^{o}N in the winter of 2000 (blue) [Schauffler et al., 2003]. While the curvature of the GMI correlations is slightly greater than Schauffler, indicating stronger mixing in the simulation, GMI N_2O and Cl_y in both hemispheres show a compact, nearly identical correlation at these levels in winter months in close agreement with the aircraft observations. This demonstrates that the Schauffler relationship can be applied to the Antarctic lower stratosphere in winter.

Next we scale the relationship measured by Schauffler et al. [2003] to account for trends in N_2O and Cl_y since 2000. To appropriately scale the relationship for each year, we increase N_2O by its observed surface growth between 2000 and 2009 of 0.77 ppb/yr [Elkins and Dutton, 2009] and decrease Cl_y by the decline projected by an updated version of the Newman et al. [2007a] EESC calculation, which estimates past and future Cl_y levels based on surface CFC measurements, CFC lifetimes, and mean ages and spectral widths appropriate for the Antarctic lower stratosphere (4.4-5.8 years and spectral width of half the mean age). This results in a Cl_y decline of 20-22 ppt/yr in the polar lower stratosphere. We demonstrate the validity of this approach by scaling the Schauffler relationship for each year from 2001-2012, then comparing these results with the GMI simulated N_2O and Cl_y for 2012, the final year used in this study which therefore has the greatest change (scaling) since 2000.

Transport produced by the MERRA meteorological fields used in the GMI CTM has realistic circulation and mixing (i.e., it produces good mean ages) and the GMI simulation uses N_2O

©2014 American Geophysical Union. All rights reserved.

Accepted Article

and CFC surface boundary conditions that change realistically during this period. If the scaling method is correct, we expect the GMI simulated N_2O/Cl_y relationship in 2012 to match the Schauffler relationship that has been scaled by 12 years of N_2O growth and Cl_y decline.

Figure 3c shows close agreement between the simulated compact correlation in 2012 (black) and the scaled Schauffler relationship (red). The agreement between the 3-dimensional global model calculation and the scaling method effectively confirms that the mean age and spectral widths used in the EESC calculation (which generates the Cl_y decline rates for the scaling) are appropriate for the Antarctic lower stratosphere. The dashed lines in Figure 3c show the sensitivity of the relationship to a ±5% variation in scaling. The simulated 2012 correlation falls completely inside this envelope, demonstrating the appropriateness of the scaling to within 5%. Figure 3d shows the scaling for the years 2004 and 2012 to illustrate the magnitude of scaling.

Note that although the scaling allows us to infer Cl_y mixing ratios from N_2O, we are primarily interested its variability. Small inaccuracies in this method have negligible impact on Cl_y variability as it is determined by the slope of the line, dCl_y/dN_2O, which changes little over the observation period. Within the N_2O 60-180 ppb range of the MLS observations used here, the slopes change by less than 15% in 12 years, thus a 10% error in the scaling would amount to little more than a 1% effect on the scaled slope and the inferred variability by 2012. A 10% bias in MLS N_2O will produce ~5% error in C_{ly} variability because dCl_y/dN_2O is nearly linear over ±10% variations in N_2O.

3.3 Inorganic Chlorine Inferred from N_2O, 2004-2012

Figure 4a shows that the same pattern of interannual variability of MLS N_2O is found on the 425, 450, and 500 K surfaces inside the Antarctic vortex. We use the appropriately scaled

©2014 American Geophysical Union. All rights reserved.

Accepted Article

Schauffler relationship for each year from 2004-2012 to calculate vortex mean inorganic chlorine using the vortex mean N_2O data shown here. The analysis is restricted to 425-500 K because the 400 K surface is sometimes below 100 hPa inside the vortex, and N_2O values above 500 K are generally below the range of the Schauffler data and dCl_y/dN_2O is small. Figure 4b presents inferred Cl_y and its interannual variability inside the Antarctic vortex during early spring ozone depletion. The black lines on the figure show projected Cl_y [Newman et al., 2007a] calculated for mean ages between 4.4 and 5.8 years (at 0.1 year intervals); these lines indicate the ranges of mean age variations on the three isentropic surfaces. Although the expected Cl_y decline due to the Montreal Protocol is 20-22 ppt per year at these mean ages, this analysis shows that Cl_y does not exhibit a monotonic decline. We find that year-to-year variations in Cl_y range from -200 ppt to +150 ppt on the 450 K surface. The transport variability that affects vortex composition causes year-to-year variability in vortex Cl_y that is nearly ten times the size of the expected annual decline due to the Montreal Protocol.

A statistically significant decline in chlorine inside the Antarctic vortex is a prerequisite for attribution of Antarctic ozone hole improvement to the impact of the Montreal Protocol. We quantify the interannual Cl_y variability using the difference between the MLS-inferred Cl_y and Cl_y calculated with the mean age appropriate for that isentropic surface [Newman et al., 2007a]. Figure 4b shows that the average mean age for Cl_y on the 450 K surface is 5.2 years. Two standard deviations (2σ) of this difference on the 450 K surface is 196 ppt (5.3% of the calculated Cl_y). The projected rate of Cl_y decline since its peak in 2000 is 20-22 ppt/year, thus 10 years (2010) is necessary to obtain a decrease in Cl_y significant at the 2σ level. The next step in attributing ozone hole recovery to the Montreal Protocol is to establish a relationship between Cl_y decline and a decrease in ozone hole area. To do this, dynamical variability [Newman et al., 2004] and the variability in Cl_y identified here must both be accounted for.

©2014 American Geophysical Union. All rights reserved.

Accepted Article

4. Cl_y, EESC, and Ozone Hole Areas from 1979-2013

The comparison of MLS-derived Antarctic Cl_y time series on three isentropic surfaces (colored lines) in Figure 4b with updated Cl_y projections from the Newman et al. [2007a] EESC calculation (black lines) shows that these surfaces have average mean ages of 4.9 ± 0.2, 5.2 ± 0.2, and 5.7 ± 0.2 yrs (2σ variation). The downward slope of these lines reflects the impact of the Montreal Protocol of -20 to -22 ppt/yr on lower stratospheric Cl_y at these mean ages during the past decade and comes from the Cl_y decline used to scale the N_2O/Cl_y relationship. In the remaining analyses we show only the 450 K results for the sake of simplicity and associate them with the EESC calculation having a mean age of 5.2 yrs, based on the results in Figure 4b. The 450 K surface, ~50-70 hPa, is a good choice for the analysis with respect to ozone hole area because temperature variations at these levels in the collar region have a large impact on chlorine activation [Newman et al., 2004].

While ozone depletion depends on Cl_y and Br_y (*i.e.*, EESC), changes in Cl_y are responsible for most of the changes in EESC since 2000. Figure 5a shows how Cl_y, EESC, and ozone hole area have varied during the period of satellite column O_3 observations, 1979-2013. (There are no NASA satellite Antarctic column O_3 data in 1995.) This figure shows calculated EESC (black line) and Cl_y (red line) using a mean age of 5.2 yrs; the MLS-derived Cl_y and EESC are shown for 2004-2012 (asterisks). 'MLS-derived' EESC for 2004-2012 was obtained by adding the Br_y time series from the Newman et al. [2007a] EESC calculation to the MLS-derived Cl_y on the 450 K surface. Transport-driven variability of Cl_y and EESC prior to 2004 is assumed to be similar to that derived here. Bromine-containing species constitute 20-25% of EESC and are mostly shorter-lived (i.e., are photolyzed at lower altitudes) than CFC-11 and CFC-12 and thus their contribution is less sensitive to transport variability in the polar lower stratosphere where mean age is > 4.5 years [Newman et al., 2007a]. The ozone hole area (blue) is calculated from NASA satellite observations of total

©2014 American Geophysical Union. All rights reserved.

Accepted Article

column O_3 less than 220 DU [Newman et al., 2004]. The area shown is an average over 11-30 September, a period when O_3 losses are high but dynamical disturbances are relatively weak. The year-to-year variations in MLS-derived Cl_y (or EESC) and area are uncorrelated because their variability has different sources. The area variability is due to the particular wave-driven dynamical disturbances that affect temperature in late winter/early spring of each year, while the Cl_y variability comes from composition variability inside the Antarctic vortex, which is strongly isolated from mixing with midlatitude air. MLS N_2O in the Antarctic middle stratosphere in fall (April) shows variability similar that found in September in the lower stratosphere, suggesting the composition variability arrived via descent within the vortex.

Figure 5a shows that EESC (and Cl_y) and area increase rapidly until the mid-1990s. After that, the relationship between EESC and area is difficult to see because year-to-year area variations are much larger than year-to-year EESC or Cl_y changes. To clarify their relationship, EESC and area are presented as a scatterplot in Figure 5b. The points from the mid-1990s to the present appear as a large cluster with EESC > 3300 ppt. All the MLS-derived EESC values are part of this cluster and are shown in blue. Although interannual variations in vortex temperature create scatter in the area, the slope of all the points in Fig. 5b suggests that even at the highest EESC levels, O_3 loss was not saturated at all locations inside the vortex where temperature was sufficiently low. Similar results are found using another ozone loss diagnostic, the ozone mass deficit (OMD). A plot of EESC against the ozone mass deficits calculated by Huck et al. [2007] for years 1979-2004 shows a generally linear relationship and slightly greater scatter (not shown).

5. The Effects of EESC and Temperature Variability on Ozone Hole Area

Since the early 1990s, any dependence of Antarctic O_3 hole area on EESC has been difficult to discern because the area varied widely, from 18-27 M km^2 (excluding 2002), while EESC varied over a relatively small range, ~3300-3900 ppt. The area variation is even larger when

©2014 American Geophysical Union. All rights reserved.

Accepted Article

2002 is included, a year with a sudden stratospheric warming that occurred in late September, unique in the Antarctic record [Allen et al., 2003]. Interannual variations in tropospheric wave driving between July and September have a strong effect on Antarctic temperatures in the collar region and are therefore a primary cause of area variability in early spring [Newman et al., 2004]. For example, the second smallest ozone hole since 1988 occurred in 2012 (19.4 M km^2) in spite of EESC levels near 3500 ppt. In late September 2012, temperatures above 20 km (~500 K) rose and caused ozone destruction to cease by early October, while temperatures below 20 km near the vortex center were low enough for destruction to continue until mid-October [Kramarova et al., 2014]. The increased temperatures above 20 km reduced ozone destruction there, leading to a larger than usual minimum column ozone (139 DU) and smaller area. Temperatures in the collar region impact area through their control of the spatial extent of polar stratospheric clouds and thus ozone loss. When they are low and dynamical disturbances are weak, the area with temperatures below the threshold for PSC formation increases. Ozone hole areas in cold years are larger because a dynamically stable vortex maintains low temperatures longer, the area of chlorine activation is larger and more persistent, and catalytic ozone destruction continues for a longer time over a larger area. In contrast to 2012, the 2006 Antarctic vortex collar region was much colder than average and the vortex was stable until mid-November [Newman et al., 2007b]. Depletion in the 14-21 km layer was larger than any previous year, EESC was within 5% of its estimated maximum value, and ozone loss rates in the 22-24 km altitude range were as large or larger than all preceding years [Hofmann et al., 2009]. The area of the 2006 ozone hole is the largest yet observed, 27.3 M km^2.

Much of the dynamical variability that has obscured the relationship between EESC and area since the early 1990s can be reduced by examining their relationship in the coldest years. We quantify temperature in the collar region, 60-75^{o}S, using 1979-2013 MERRA temperatures to

©2014 American Geophysical Union. All rights reserved.

Accepted Article

calculate their area-weighted mean for 11-30 September each year on the 31, 52, 73, and 100 hPa levels. This is similar to the temperature proxy used by Newman et al. [2006] in their parametric model of ozone hole area. Figure 6a shows the temperature anomaly with respect to the mean for each pressure level expressed in standard deviations from the mean. Five years stand out by having temperatures ~1σ below the mean on all four levels: 1987, 1998, 2006, 2008, and 2011.

We use this temperature metric to sort the EESC and area data by collar temperature for years with areas > 15 M km^2. In Figure 6b, the years with collar temperatures at or above the 35-yr mean at all four levels are shown in red, while years that are 0.9σ or more below the mean at all four levels are shown in blue. All other years are shown in green. The EESC values from 2004-2012 are the MLS-derived values. The 1σ variability of the inferred Cl_y (2.67%) is used to approximate EESC variability in all other years and is shown by the vertical bar. The warm years are mostly along the left side of the envelope of points, producing small areas for their EESC values. The coldest years fall on the right side of the plot, produce the largest areas for their EESC level, and show a linear relationship (dashed line). Date ranges spanning 2 to 5 weeks between 7 September and 13 October produced similar results, and a temperature metric calculated for 60-90^{o}S instead of 60-75^{o}S identified the same warm and cold years. Use of the temperature metric to identify very cold years reduces the effect of temperature variations on area, revealing the underlying relationship between EESC and area.

The three years following the 1991 Pinatubo eruption also have large areas for their EESC level, much like the coldest years. South Pole ozone sondes showed there was unusual depletion in the lowermost stratosphere (12-14 km, <380 K) in 1992-1994 due to increased aerosol surface area, resulting in an estimated additional 10-15 DU loss in these years [Hofmann et al., 1997]. A similar increase in column O_3 loss below 400 K was reported for the Arctic winter of 1991-92 [Tilmes et al., 2008]. Rex et al. [2004] found that the increased

©2014 American Geophysical Union. All rights reserved.

Accepted Article

polar O_3 loss due to Pinatubo aerosols correlated linearly with the log of the aerosol surface area density.

Figure 6 shows that a clear, linear relationship between EESC and area is found when temperature variability is greatly reduced. For the years with well-below average collar temperature throughout the 30-100 hPa region, greater EESC produced larger ozone hole areas. The relationship between EESC and area in these years suggests that future ozone holes will continue to be larger than 20 M km^2 in cold years as long as EESC levels are above ~2850 ppt; this is roughly the 1987 EESC level.

Ironically, it may be that the largest ozone holes of recent years rather than the smaller ones (e.g., 2010 and 2012) provide evidence for an ozone response to declining Cl_y levels. The largest Antarctic ozone hole occurred in 2006 and was one of the coldest years of the 35-year record. The linear relationship between EESC and area in the coldest collar years suggests that the smaller areas in 2008 and 2011, also two of the coldest years, are a response to declining EESC. This would not be apparent without the MLS-derived EESC values. Compared to the MLS-derived quantities, EESC from the Newman et al. [2007a] calculation is 37 ppt lower in 2006, 51 ppt higher in 2008, and 130 ppt higher in 2011. The line created by these points (not shown) runs through 1991, a year with above average collar temperatures. The relationship between MLS-derived EESC and area in the recent cold years suggests that the maximum area possible each year depends on EESC.

Based on the historical ozone hole area record shown in Fig. 5a, the projected decline in EESC due to the Montreal Protocol, and the interannual variability of Antarctic lower stratospheric Cl_y found in this study, we estimate the date when the ozone hole area will be consistently smaller than 20 M km^2. The smoothly declining EESC shown in Figure 7 drops below 2850 ppt in 2037, but when considering the effect of $\pm 1\sigma$ Cl_y variability (98 ppt), this value may occur several years later. At present, ozone holes smaller than 20 M km^2 occur

©2014 American Geophysical Union. All rights reserved.

Accepted Article

when the vortex is disturbed and collar temperatures are not especially low or enduring. In the absence of enhanced aerosol surface area in the Antarctic lower stratosphere, all ozone holes after the 2030s are likely to be smaller than 20 M km^2 regardless of temperature and dynamics. This is compatible with the projected decline in Antarctic O_3 loss rates reported by Hassler et al. [2011]. Using the Newman calculation of EESC decline for a mean age of 5.5 years, they found that a statistically significant decrease in O_3 loss rates should occur at all levels between 100-20 hPa by 2030.

6. Conclusions and Summary

MLS N_2O observations from 2004-2012 reveal large interannual composition variability inside the Antarctic lower stratospheric vortex. Using the compact correlation between N_2O and Cl_y derived from observations in 2000, scaled to account for increased N_2O and decreased CFC abundances since that time, we used MLS N_2O to infer the interannual variability of inorganic chlorine in the Antarctic vortex. The transport variability causing the observed variations in vortex composition also affects ozone hole area through its impact on Cl_y levels inside the vortex. The downward trend in the 9-yr Cl_y record is imposed by the projected decline due to the Montreal Protocol (~220 ppt/decade) that is inherently part of the scaling method used to infer Cl_y from N_2O, but the year-to-year variability in Cl_y comes from the MLS N_2O variability with little sensitivity to the scaling. The inferred 2σ Cl_y variability, 196 ppt, is roughly ten times larger than the imposed annual decline since 2000 of 20-22 ppt/year. This means roughly 10 years are required for a significant chlorine trend inside the Antarctic lower stratospheric vortex attributable to the Montreal Protocol.

The magnitude of this geophysical variability effectively prohibits attribution of O_3 hole area reduction to the Montreal Protocol earlier than 2010, 10 years after observations began to show declining stratospheric Cl_y [Rinsland et al., 2003; Froidevaux et al., 2006]. Accounting only for dynamical variability, Salby et al. [2011] report an upward trend in Antarctic column

©2014 American Geophysical Union. All rights reserved.

Accepted Article

ozone since 2000 that they attribute to declining CFCs. Our results demonstrate that both temperature (i.e., dynamics) and Cl_y variability must be accounted for in attributing the cause of ozone hole area variations, casting doubt on their attribution that accounted for dynamical variability alone.

While projected EESC calculated by Newman et al. [2007a] should be accurate in the mean because it is based on recent surface observations, updated stratospheric lifetimes for ODSs [SPARC, 2013], observed fractional releases, and realistic assumptions about the age spectrum in polar regions, it contains no information on the transport variability that affects vortex composition, i.e., Cl_y, in any given year. We found that year-to-year variability in vortex Cl_y is equivalent to moving forward or backward by as much as 7 years on the EESC curve (Fig. 7). The observationally-derived estimates of Cl_y (and EESC) give us a clearer understanding of how area and Cl_y will vary in the coming decades as the Montreal Protocol continues to reduce halogen loading.

The historical record shows a clear dependence of ozone hole area on Cl_y before 1992 when Cl_y levels were rapidly increasing. Since then, Cl_y changes have been small, and dynamically-driven variations in temperature have dominated the area variations. We find a clear and linear relationship between ozone hole area and EESC in years when Antarctic collar temperatures were one standard deviation or more below the 35-year mean at levels 30-100 hPa in late September. The relationship between EESC and area in the coldest years suggests that ozone holes larger than 20 M km^2 will continue to occur in very cold years until EESC levels return to ~2850 ppt, the level calculated for 1987. Given the projected rate of EESC decline and the observed Cl_y variability of the past decade, we expect EESC to consistently be at or below this level after 2040. At current EESC levels, years with a dynamically disturbed vortex and above average lower stratospheric temperatures can result in an ozone hole area of less than 20 M km^2. In the absence of enhanced volcanic aerosol loading, EESC

©2014 American Geophysical Union. All rights reserved.

Accepted Article

levels in 2040 and beyond are likely to produce ozone hole areas less than 20 M km^2 regardless of dynamics. Declining EESC levels make it unlikely that any future ozone holes will be as large as 2006.

Acknowledgments. This work was supported by the NASA Modeling, Analysis, and Prediction Program and the NASA Atmospheric Composition Modeling and Analysis Program. MLS data are available at http://mls.jpl.nasa.gov. GMI simulation output is available by request to susan.e.strahan@nasa.gov. We thank Eric Nash for providing column O_3 measurements on the NASA Ozone Watch website, http://ozonewatch.gsfc.nasa.gov/meteorology/annual_data.html. We genuinely appreciate the insightful and constructive comments from the reviewers.

References

Allen, D.R., R.M. Bevilacqua, G.E. Nedoluha, C.E. Randall, and G.L. Manney, (2003), Unusual stratospheric transport and mixing during the 2002 Antarctic winter, Geophys. Res. Lett., 30, doi:10.1029/2003GL017117.

Bodeker, G.E., H. Shiona, and H. Eskes (2005), Indicators of Antarctic ozone depletion, Atmos. Chem. Phys., 5, 2603-2615.

Daniel, J., S. Solomon, and D.L. Albritton (1995), On the evaluation of halocarbon radiative forcing and global warming potentials, J. Geophys. Res., 100, 1271-1285.

Elkins, J.W, and G.S. Dutton (2009), Nitrous oxide and sulfur hexafluoride [in 'State of the Climate in 2008']. Bull. Amer. Meteor. Soc, 90, S38-S39.

Farman, J. C., B. G. Gardiner, and J. D. Shanklin (1985), Large losses of total ozone in Antarctica reveal seasonal ClO_x/NO_x interaction, Nature, 315, 207– 210.

Froidevaux, L., N.J. Livesey, W.G. Read, R.J. Salawitch, J.W. Waters, B. Drouin, I.A. MacKenzie, H.C. Pumphrey, P. Bernath, C. Boone, R. Nassar, S. Montzka, J. Elkins, D.

©2014 American Geophysical Union. All rights reserved.

Accepted Article

Cunnold, and D. Waugh (2006), Temporal decrease in upper atmospheric chlorine, Geophys. Res. Lett., 33, doi:10.1029/2006GL027600.

Hall, T.M., D.W. Waugh, K.A. Boering, and R.A. Plumb (1999), Evaluation of transport in stratospheric models, J. Geophys. Res., 104, 18,815-18,839.

Hassler, B., J. S. Daniel, B. J. Johnson, S. Solomon, and S. J. Oltmans (2011), An assessment of changing ozone loss rates at South Pole: Twenty-five years of ozonesonde measurements, J. Geophys. Res., 116, doi:10.1029/2011JD016353.

Hofmann, D. J., S. J. Oltmans, J. M. Harris, B. J. Johnson, and J. A. Lathrop (1997), Ten years of ozonesonde measurements at the south pole: Implications for recovery of springtime Antarctic ozone, J. Geophys. Res., 102, 8931– 8943.

Hofmann, D.J., B.J. Johnson, and S. J. Oltmans (2009), Twenty-two years of ozonesonde measurements at the South Pole, Intl. J. Rem. Sens., 30, 3995-4008.

Huck, P. E., S. Tilmes, G. E. Bodeker,W. J. Randel, A. J. McDonald, and H. Nakajima (2007), An improved measure of ozone depletion in the Antarctic stratosphere, J. Geophys. Res., 112, D1110, doi:10.1029/2006JD007860.

Kawa, S.R., D.W. Fahey, L.E. Heidt, W.H. Pollock, S. Solomon, D.E. Anderson, M. Loewenstein, M.H. Proffitt, J.J. Margitan, and K.R. Chan (1992), Photochemical partitioning of the reactive nitrogen and chlorine reservoirs in the high-latitude stratosphere, J. Geophys. Res., 97, 7905-7923.

Kawa, S.R., P.A. Newman, L.R. Lait, M.R. Schoeberl, R.M. Stimpfle, D.W. Kohn, C.R. Webster, R.D. May, D. Baumgardner, J.E. Dye, J.C. Wilson, K.R. Chan, and M. Loewenstein (1997), Activation of chlorine in sulfate aerosol as inferred from aircraft observations, J. Geophys. Res., 102, 3921-3933.

Accepted Article

©2014 American Geophysical Union. All rights reserved.

Kramarova, N. A., E.R. Nash, P.A. Newman, P.K. Bhartia, R.D. McPeters, D.F. Rault, C.J. Seftor, P.Q. Xu, G. Labow (2014), Measuring the Antarctic ozone hole with the new Ozone Mapping and Profiler Suite (OMPS), Atmos. Chem. Phys., 14, 2353-2361.

Lambert, A., et al. (2007), Validation of the Aura Microwave Limb Sounder middle atmosphere water vapor and nitrous oxide measurements, J. Geophys. Res., 112, D24S36, doi:10.1029/2007JD008724.

Livesey, N., et al. (2011), Earth Observing System (EOS) Aura Microwave Limb Sounder (MLS) Version 3.3 Level 2 data quality and description document, JPL D-33509.

Nash, E.R., P.A. Newman, J.E. Rosenfield, and M.R. Schoeberl (1996), An objective determination of the polar vortex using Ertel's potential vorticity, J. Geophys. Res., 101, 9471-9478.

Newman, P.A., S.R. Kawa, and E.R. Nash (2004), On the size of the Antarctic ozone hole, Geophys. Res. Lett., 31, L21104, doi:10.1029/2004GL020596.

Newman, P.A., E.R. Nash, S.R. Kawa, S.A. Montzka, and S.M. Schauffler (2006), When will the Antarctic ozone hole recover?, Geophys. Res. Lett., 33, L12814, doi:10.1029/2005GL025232.

Newman, P.A., J.S. Daniel, D.W. Waugh, and E.R. Nash (2007a), A new formulation of equivalent effective stratospheric chlorine (EESC), Atmos. Chem. Phys., 7, 4537-4552.

Newman, P.A., B.J. Johnson, D. Lubin, S.J. Oltmans, and R.C. Schnell (2007b), 2006 Austral springtime ozone depletion [in 'State of the Climate in 2006']. Bull. Amer. Meteor. Soc, 88, S75-S77.

Plumb, R. A. (2007), Tracer interrelationships in the stratosphere, Res. Geophys., 45, RG4005, doi:10.1029/2005RG000179.

©2014 American Geophysical Union. All rights reserved.

Accepted Article

Plumb, R.A. and M.K.W. Ko (1992), Interrelationship between mixing ratios of long-lived stratospheric constituents, J. Geophys. Res., 97, 10,145-10,156.

Rex, M., R. J. Salawitch, P. von der Gathen, N. R. P. Harris, M. P. Chipperfield, and B. Naujokat (2004), Arctic ozone loss and climate change, Geophys. Res. Lett., 31, L04116, doi:10.1029/2003GL018844.

Rienecker, M.M. et al. (2011), MERRA: NASA's Modern Era Retrospective Analysis for Research and Applications, J. Climate, 24, 3624-3648.

Rinsland, C.P., E. Mahieu, R. Zander et al. (2003), Long-term trends of inorganic chlorine from ground-based infrared solar spectra: Past increases and evidence for stabilization, J. Geophys. Res., 108, 4252, doi:10.1029/2002JD003001.

Salby, M., E. Titova, and L. Deschamps (2011), Rebound of Antarctic ozone, Geophys. Res. Lett., 38, L09702, doi:10.1029/2011GL047266.

Schauffler, S. M., E.L. Atlas, S.G. Donnelly, A. Andrews, S.A. Montzka, J.W. Elkins, D.F. Hurst, P.A. Romashkin, G.S. Dutton, and V. Stroud (2003), Chlorine budget and partitioning during the Stratospheric Aerosol and Gas Experiment (SAGE) III Ozone Loss and Validation Experiment (SOLVE), J. Geophys. Res., 108(D5), 4173, doi:10.1029/2001JD002040.

SPARC (2010), Report on the Evaluation of Chemistry-Climate Models, V. Eyring, T.G. Shepherd, D.W. Waugh (Eds.), SPARC Report No. 5, WCRP-132, WMO/TD-No. 1526.

SPARC (2013), Report on the Lifetimes of Stratospheric Ozone-Depleting Substances, Their Replacements, and Related Species, M. Ko, P. Newman, S. Reimann, S. Strahan (Eds.), SPARC Report No. 6, WCRP-15/2013.

Accepted Article

©2014 American Geophysical Union. All rights reserved.

Strahan, S.E., M. Loewenstein, and J.R. Podolske (1999), Climatology and small-scale structure of lower stratospheric N_2O based on in situ observations, J. Geophys. Res., 104, 2195-2208.

Strahan, S.E., et al. (2011), Using transport diagnostics to understand chemistry climate model ozone simulations, J. Geophys. Res., 116, doi:10.1029/2010JD015360.

Strahan, S. E., A.R. Douglass, and P.A. Newman (2013), The contributions of chemistry and transport to low Arctic ozone in March 2011 derived from Aura MLS observations, J. Geophys. Res., 118, 1563–1576, doi:10.1002/jgrd.50181.

Strong, K., et al. (2008), Validation of ACE-FTS N_2O measurements, Atmos. Chem. Phys., 8, 4759-4786.

Tilmes, S., R. Mueller, R. J. Salawitch, U. Schmidt, C. R.Webster, H. Oelhaf, J. M. Russell III, and C. C. Camy-Peyret (2008), Chemical ozone loss in the Arctic winter 1991–1992, Atmos. Chem. Phys., 8, 1897–1910.

Uchino, O., R.D. Bojkov, D.S. Balis, K. Akagi, M. Hayashi, and R. Kajihara (1999), Essential characteristics of the Antarctic-spring ozone decline: Update to 1998, Geophys. Res. Lett., 26, 1377-1380.

Waugh, D.W., S.E. Strahan, and P.A. Newman (2007), Sensitivity of stratospheric inorganic chlorine to differences in transport, Atmos. Chem. Phys., 7, 4935-4941.

Woodbridge, E.L. et al. (1995), Estimates of total organic and inorganic chlorine in the lower stratosphere from in situ and flask measurements during AASE II, J. Geophys. Res., 100, 3057-3064.

World Meteorological Organization (WMO) (2003), Scientific assessment of ozone depletion: 2002, Global Ozone Res. Monit. Proj. Rep. 47, Geneva, Switzerland.

©2014 American Geophysical Union. All rights reserved.

Accepted Article

Accepted Article

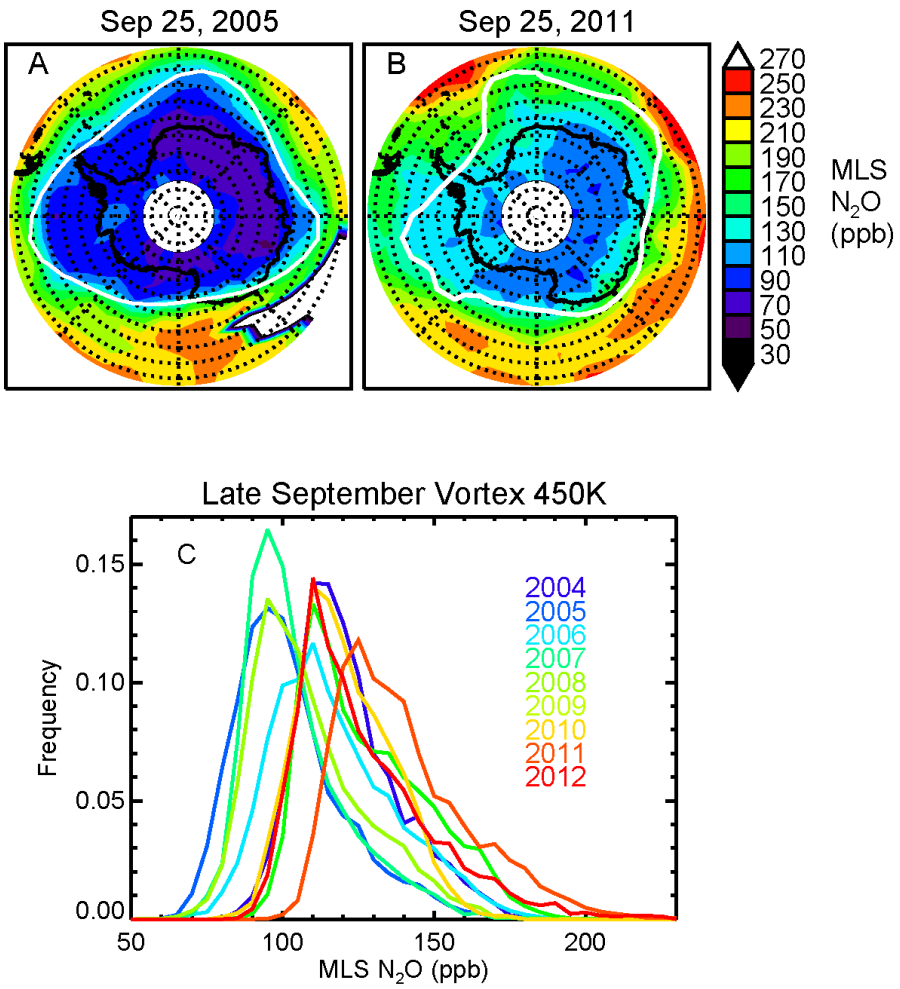

Figure 1. MLS N_2O on the 450 K isentropic surface on A) September 25, 2005 and B) September 25, 2011. The 450 K vortex edge (the -4.0 x 10^{-5} K m^2/kg s potential vorticity contour) is shown in white. C) MLS N_2O frequency distributions inside the Antarctic vortex on the 450 K surface, averaged 21-30 September each year, 2004-2012.

©2014 American Geophysical Union. All rights reserved.

Accepted Article

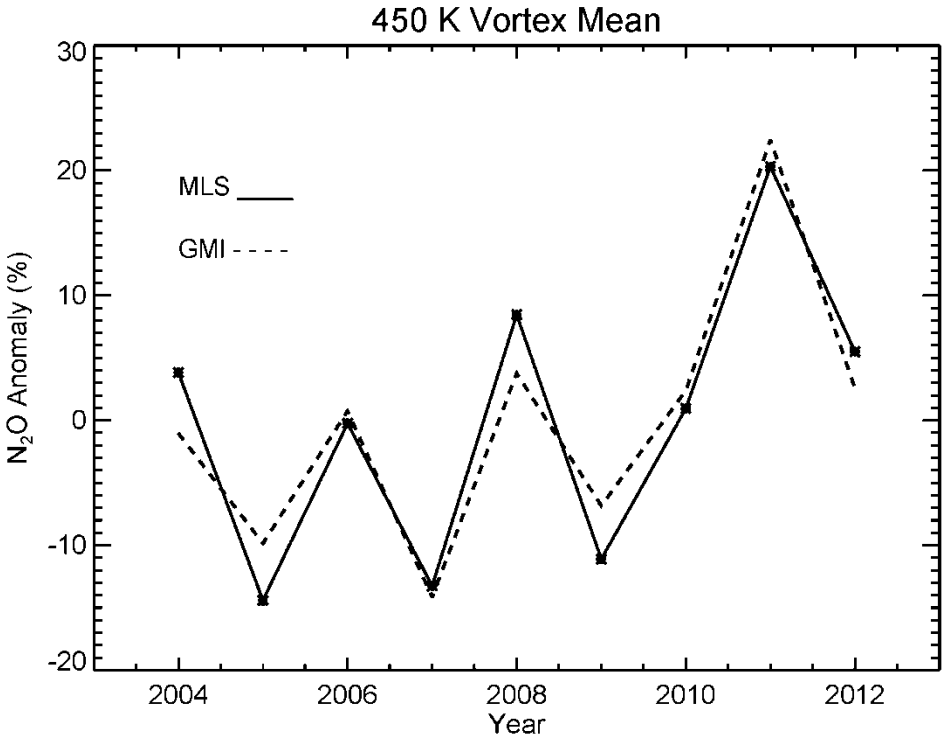

Figure 2. Comparison of 450 K vortex mean N_2O anomalies, 21-30 September 2004-2012, calculated from MLS observations (solid) and the GMI simulation using MERRA meteorology (dashed). The correlation between the time series is 0.95.

©2014 American Geophysical Union. All rights reserved.

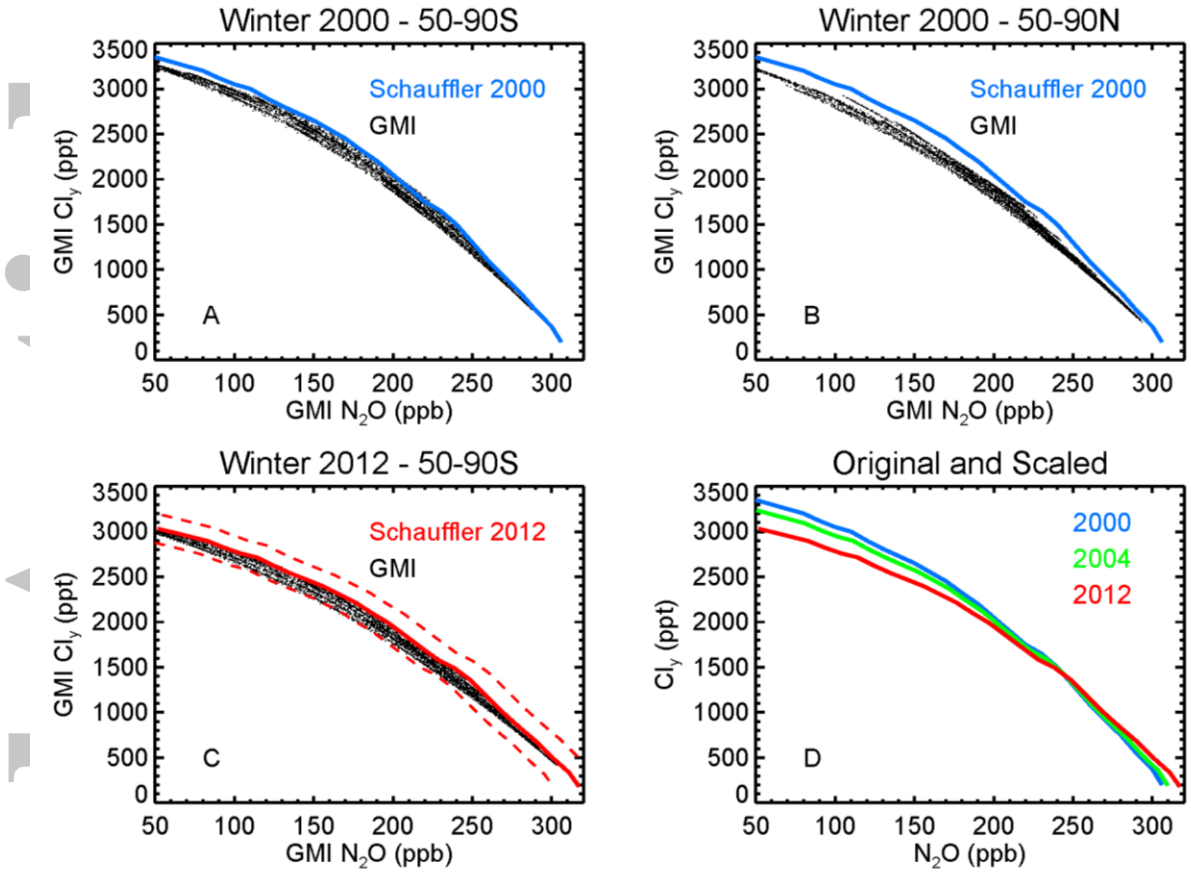

Figure 3. N_2O and Cl_y from the GMI CTM (black) compared to the Schauffler relationship (blue) from 2000, 52-88°N: A) GMI Antarctic winter 2000, B) and GMI Arctic winter 2000. Model points are from isentropic surfaces 400-500 K. C) GMI Antarctic winter 2012 compared to the Schauffler relationship scaled for 2012 (red) and ±5% scaling variation. D) Comparison of the original Schauffler relationship (blue) and the scaled relationships for 2004 and 2012 showing the range of scaling required for Aura time period.

Accepted

©2014 American Geophysical Union. All rights reserved.

Accepted Article

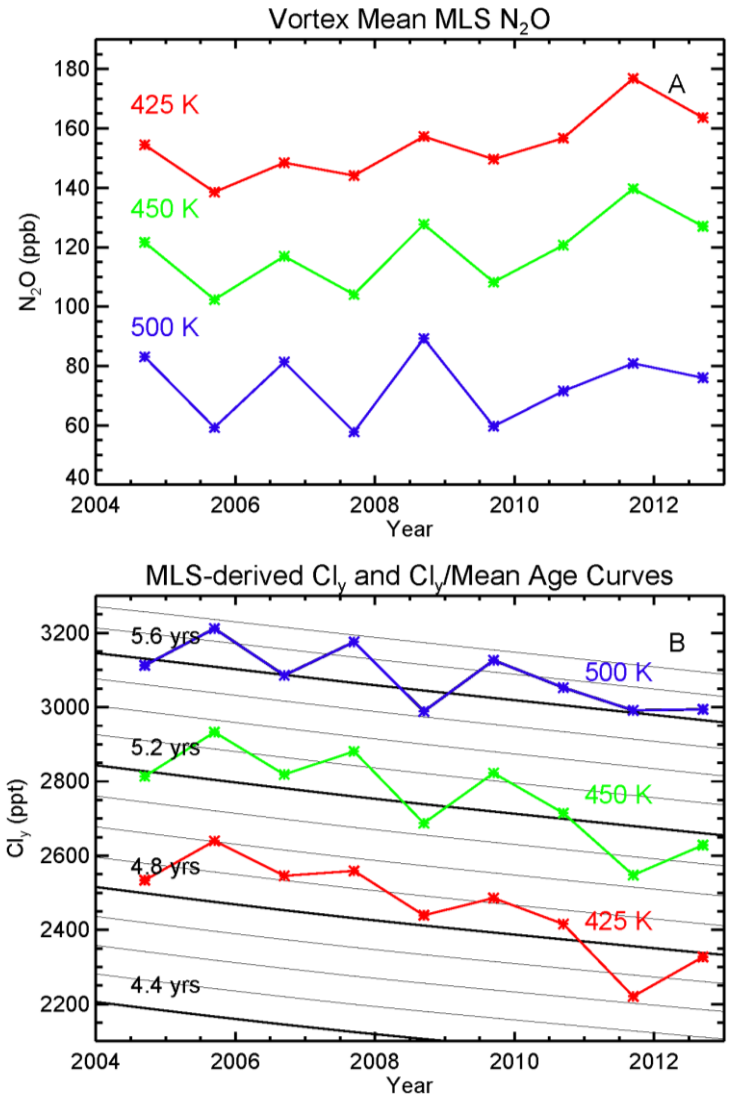

Figure 4. A) Antarctic vortex mean MLS N_2O, 2004-2012, on three lower stratospheric isentropic surfaces. B) Based on the scaled Schauffler relationship, MLS-derived Cl_y in the Antarctic vortex on the same three isentropic surfaces for late September of each year. The thin and thick black lines are the projected Cl_y time series for mean ages between 4.4 and 5.8 years (0.1 year intervals) from the Newman et al. [2007a] calculation.

©2014 American Geophysical Union. All rights reserved.

Accepted Article

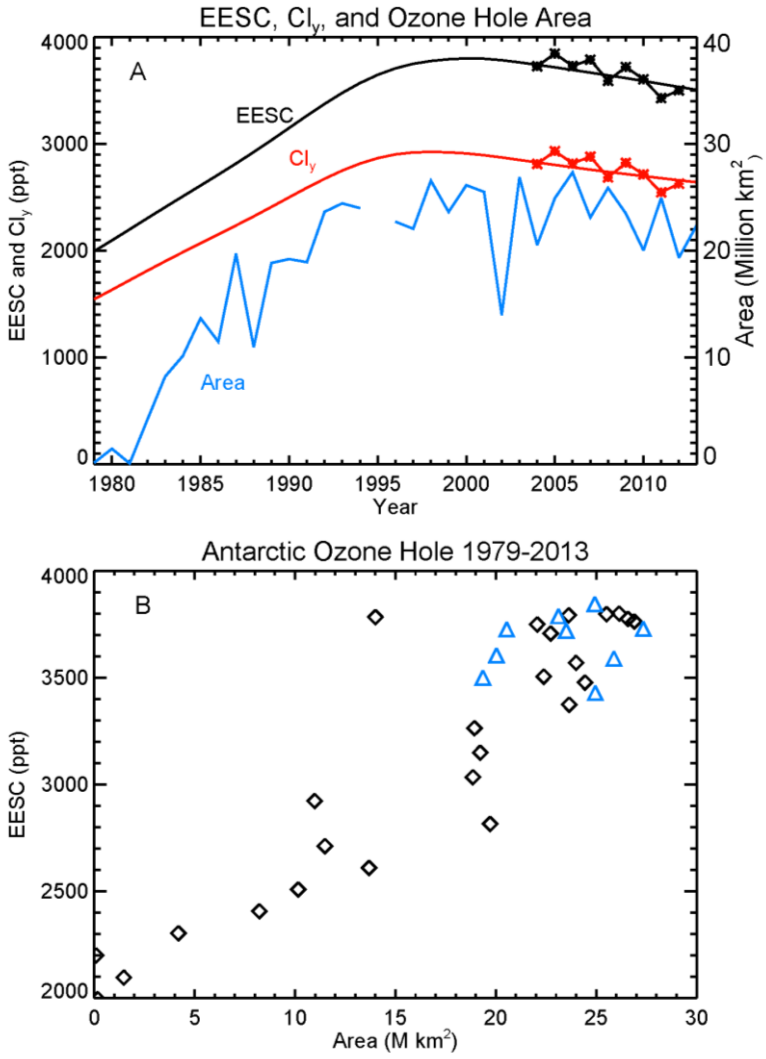

Figure 5. A) EESC (black line) and Cl_y (red line) for 1979-2013 from the Newman calculation with mean age 5.2 yrs (approximately 450 K). MLS-derived Cl_y from this study (red asterisks) and MLS-derived EESC (black asterisks), calculated from MLS-derived Cl_y and projected Br_y [Newman et al. 2007a], are shown for 2004-2012. Ozone hole area averaged 11-30 September is shown in blue. B) Scatterplot of the EESC and area data shown in A). MLS-derived EESC values are shown with blue triangles.

©2014 American Geophysical Union. All rights reserved.

Accepted Article

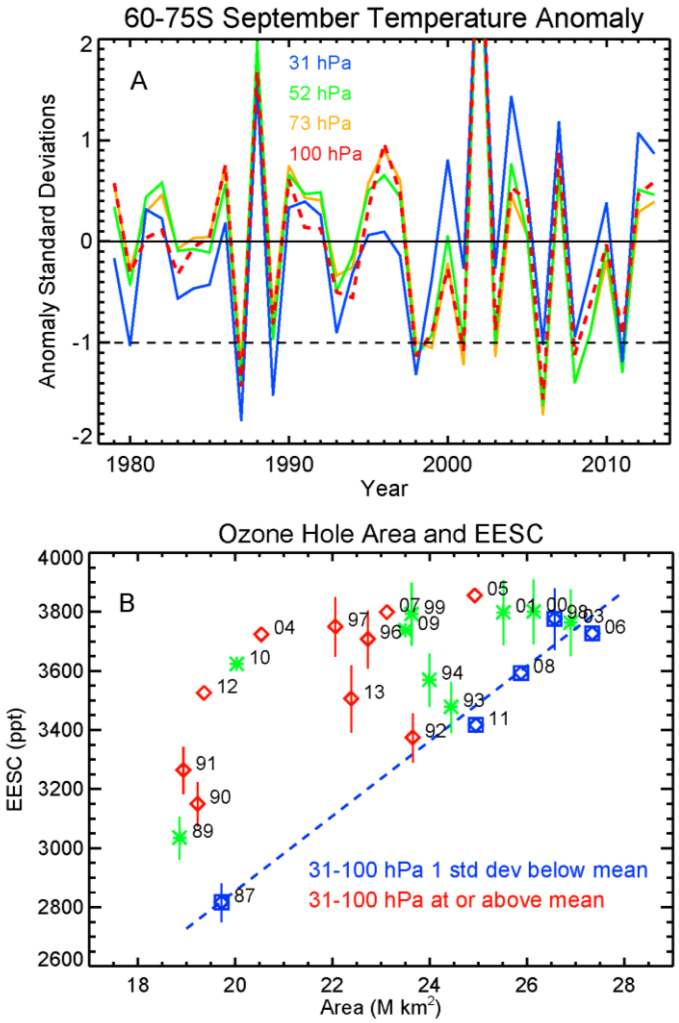

Figure 6. A) Antarctic collar temperature anomalies, 31-100 hPa, based on MERRA zonal mean temperatures averaged over 11-30 September, 1979-2013. For each pressure level the anomaly with respect to the 35-yr mean is expressed in units of standard deviation. B) EESC and area data from Figure 5 for all years with area >15 M km^2. Blue points are the years where collar temperatures were about 1σ or more below the mean at all levels, 31-100 hPa. The dashed blue line shows the linear relationship between EESC and area in the coldest years. Red diamonds are the years with temperature at or above the mean. All other years are shown with green asterisks. The vertical bars, shown for years outside of 2004-2012, indicate the estimated 1σ uncertainty in EESC based on the inferred Cl_y variability at 450 K (Fig. 4b).

©2014 American Geophysical Union. All rights reserved.

Accepted Article

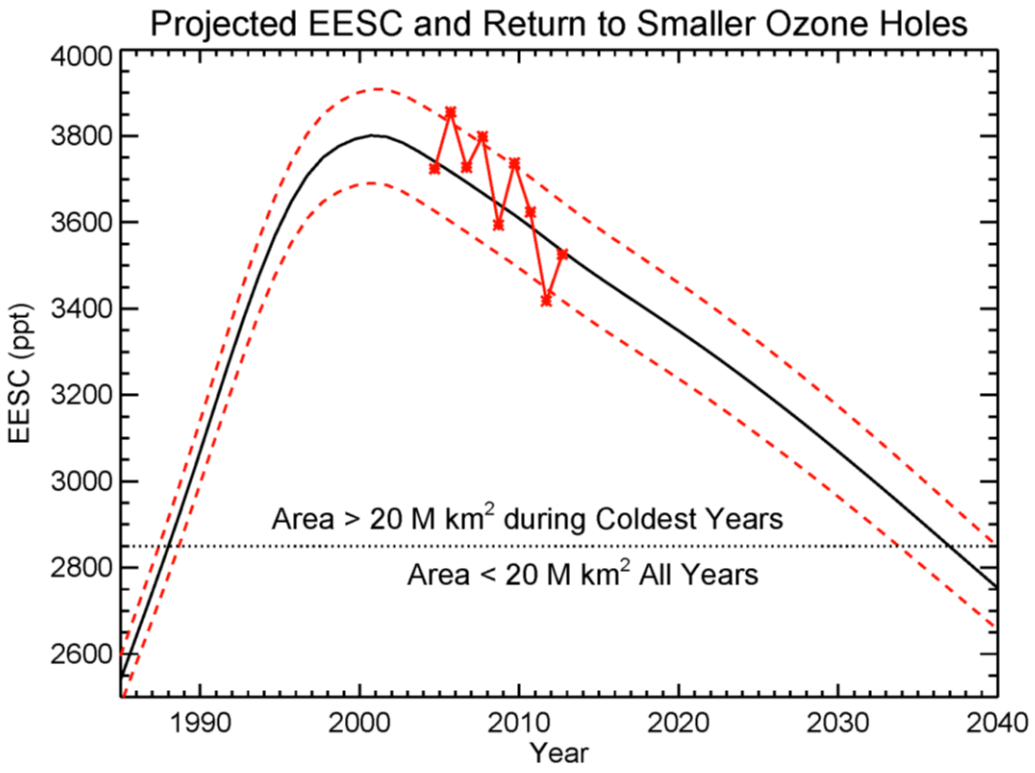

Figure 7. Estimated past and projected future EESC (black line) and MLS-derived EESC, 2004-2012 (red asterisks). The dashed red lines show the estimated 1σ EESC variability based on 9 years of MLS-derived Cl_y.

©2014 American Geophysical Union. All rights reserved.